

Oxide Electronics Transferred on Stiff-Stripe/ PDMS Substrate for High-Resolution Stretchable Displays

Xiuling Li, Md. Mehedi Hasan[✉], Hyo-Min Kim, and Jin Jang[✉], *Member, IEEE*

Abstract—We report flexible oxide semiconductor-based electronics transferred on polydimethylsiloxane (PDMS) elastomer substrate in the form of stiff stripes for stretchable displays. Stiff stripes with optimized geometries are placed between PDMS substrate and oxide electronics to provide strong adhesion and mechanical protection. Amorphous indium–gallium–zinc oxide (a-IGZO) thin-film transistors (TFTs) and gate driver circuits on polyimide substrate are cut into identical stripe shape and transferred onto the stiff region. The turn-on voltage (V_{ON}) and mobility of the fabricated a-IGZO TFTs vary within ± 0.4 V and 7.4%, respectively, after 50% stretching and relaxation for 1000 cycles. The circuits on the stiff-stripe/elastomer substrate can be repeatedly stretched to 50% without mechanical and electrical degradations. The results can be used for practical stretchable displays with high resolution over a large area.

Index Terms—Amorphous indium–gallium–zinc oxide (a-IGZO) thin-film transistor (TFT), circuits, polydimethylsiloxane (PDMS), stiff stripes, stretchable.

I. INTRODUCTION

DISPLAY devices that offer mechanical flexibility and stretchability can enable intimate integration into daily life such as smart textiles and healthcare monitors, where heavy and rigid origins are no longer qualified [1], [2]. Extremely bendable or foldable displays (bending radii in millimeter scales) have been achieved using ultrathin substrates, durable functioning layers, or tuning of the neutral mechanical plane [3]–[6]. However, stretchability is more demanding than flexibility. One of the key challenges is to tolerate much higher levels of strains (typically $>10\%$) without fracture or significant degradation in electrical functionalities [7]–[9]. Although there have been remarkable results on intrinsically stretchable

materials, the mass production of these devices and electronics needs further study [10]. Current displays generally employ inorganic materials such as amorphous oxide semiconductors (AOSs) or silicon-based alternatives, which are brittle with fracture strains of less than 2% [11], [12]. This needs the implementation of strain relieves through mechanical designs and maintaining high compatibility with mature display fabrication processes.

Mechanical structures such as wrinkling/buckling and stiff patches have been widely explored to dissipate the induced strain during large deformation. The wrinkled/buckled structures formed by the relaxation of prestretched substrates after complete device fabrication have been widely employed in numerous stretchable sensors and energy devices [13]. However, such structures introduce large tensile/compressive strains through micrometer-scale bending radii, associated with complex and nonlinear forming physics [14]–[16]. In addition, corrugation on the surface is less desirable for displays [17]. Stiff patches (Young's modulus E in GPa range) provide mechanical protections on flat surfaces when the elastomer substrate is macroscopically stretched. The brittle inorganic components with high electrical performance can be stretched to $\gg 10\%$ [7]. The use of stiff patches, therefore, has been considered as one of the most promising methods to achieve stretchable displays.

Numerous studies have alternatively reported on stiff patches either embedded in, directly deposited, or transferred on the elastomer substrate. Materials forming the stiff region vary from polyimide (PI, $E_{PI} = 2.54$ GPa) [18]–[21] polyethylene terephthalate (PET, $E_{PET} = 2$ – 2.7 GPa) [22], diamond-like carbon (DLC, $E_{DLC} > 200$ GPa) [23], and SU-8 ($E_{SU-8} = 4$ GPa) [24] to complex multilayered structures with mechanical gradients for optimizing adhesion and strain distribution [7], [11], [23]. In recent works, electronic devices are transferred onto stiff islands and are interconnected by stretchable conductors [17]–[25]. In addition to avoid the thermal/chemical stability issues from direct fabrication on elastomers, transfer technique can employ high-performance electrical devices with the effort of additional transfer steps from conventional substrates [1], [17], [25]. However, this technique can be possible by transferring a single device or pixel onto each island-shaped stiff region.

Manuscript received April 1, 2019; accepted May 15, 2019. Date of publication June 5, 2019; date of current version June 19, 2019. This work was supported in part by the Ministry of Trade, Industry and Energy (MOTIE) under Grant 10052044 and in part by Korea Display Research Corporation (KDRC) through the program for the Development of Future Device Technology for the Display Industry. The review of this paper was arranged by Editor X. Guo. (Corresponding author: Jin Jang.)

The authors are with the Department of Information Display, Advanced Display Research Center, Kyung Hee University, Seoul 130-701, South Korea (e-mail: jjang@khu.ac.kr).

Color versions of one or more of the figures in this paper are available online at <http://ieeexplore.ieee.org>.

Digital Object Identifier 10.1109/TED.2019.2918160

The yield of transfer processes becomes challenging for large-area and high-pixel-density displays.

Here, we propose a concept involving the transfer of oxide thin-film transistor (TFT)-based flexible electronics onto stiff stripes on polydimethylsiloxane (PDMS) elastomer substrate. In contrast to the previous reports, each stiff platform in a stripe shape is proposed to support a small functional display which can be integrated with high-performance TFT-based gate driver and active pixels, and thus the transfer process is possible with high fabrication yield. The stiff stripes, made of commercially available adhesive tape, are cut into optimized geometries and are placed between electronics and PDMS substrate. The function of the stiff stripes includes providing strong adhesion and mechanical protection of the brittle electronics. As a proof-of-concept study, oxide TFTs and circuits (inverter and gate driver) on the flexible PI substrate are cut into identical stripe shape and transferred onto the stiff region to test stretchability and robustness. As the representative of oxide TFTs, amorphous indium–gallium–zinc oxide (a-IGZO) TFT was chosen herein since it has been considered the most favorable device for display applications due to its relatively high field-effect mobility ($>10 \text{ cm}^2/\text{V}\cdot\text{s}$), excellent electrical stability, superior scalability, and low-temperature process [26]. The fabricated a-IGZO TFTs and gate driver circuits are exposed to 50% repeated stretching without significant degradation in mechanical and electrical properties.

II. EXPERIMENT

The a-IGZO TFTs and circuits were initially fabricated on a flexible PI substrate. The stripe-shaped electronics membranes were formed by using high-resolution laser cutting. Two-times transfer process was performed to make the stretchable electronics. The stiff stripes were first transferred (first transfer) onto PDMS elastomer substrate. Then, the flexible electronics with identical stripe shape were transferred (second transfer) onto the stiff region. The preparation process is described in the following.

A. Preparation of Stiff Stripes on PDMS Substrate

The preparation of stiff stripes on a PDMS substrate was started with a double-sided adhesive tape (Kapton DuPont) that was cut into 30-mm-long stripes with widths varying from 1 to 3 mm. The thickness, peel adhesion, and E of the adhesive tape are $\sim 150 \mu\text{m}$ (25- μm -thick stiff layer sandwiched by $\sim 60\text{-}\mu\text{m}$ -thick adhesive layers on both sides), 120 N/25 mm, and 2–2.5 GPa, respectively. Fig. 1 shows the schematic (left) and photographs (right) of the preparation process. PDMS was chosen as a stretchable substrate due to its excellent stretchability, high transparency, and good compatibility with human skins [27]. PDMS solution was prepared by mixing a silicone gel and a cross-linker with a weight ratio of 10:1 (Sylgard 184; Dow Corning). After depositing a mixture of carbon nanotubes (CNTs)/graphene oxide (GO) on a carrier glass, the PDMS substrate was prepared by spin coating, thermally cured at 150 °C for 15 min, and then peeled off from the glass carrier [Fig. 1(a)]. The very thin CNT/GO was

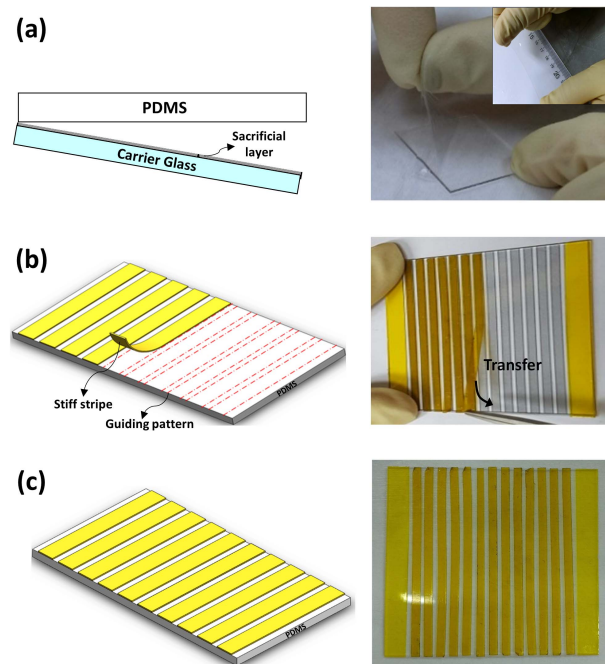


Fig. 1. Preparation of stiff stripes on the PDMS substrate. (a) Schematic and photograph showing the preparation of the stretchable PDMS substrate. Inset: highly transparent and stretchable PDMS after being peeled off from the glass carrier. (b) Transfer of stiff stripes onto the PDMS substrate using the pick-and-place method. Stripe patterns are put underneath PDMS to guide the transfer. (c) Stiff-stripe/PDMS substrate after the complete process.

used as a sacrificial layer to reduce the peel strength [3]. Fig. 1(b) shows the transfer of stripe-shaped adhesive tapes onto the PDMS substrate using the pick-and-place method. The stripes with identical width were transferred onto the PDMS substrate with fixed spacing. Drawn stripe patterns were placed underneath the PDMS substrate to guide for accurate transfer. Fig. 1(c) shows the stiff-stripe/PDMS substrate after the complete transfer process.

B. Fabrication of Stretchable a-IGZO TFTs

Fig. 2(a)–(d) shows the key steps to prepare a-IGZO TFTs on the stiff-stripe/PDMS substrate. First, flexible a-IGZO TFTs on the PI substrate were fabricated [Fig. 2(a)]. Second, the TFT membrane was cut into a stripe shape using a green laser [Fig. 2(b)]. Third, the stripe-shaped TFT membranes were subsequently transferred onto the stiff region on the PDMS substrate [Fig. 2(c) and (d)]. To maintain the high yield of the transfer process, wrinkling- or curling-free oxide TFTs on PI are of great importance. The flexible devices were initially fabricated on PI/glass substrate and subsequently detached from the glass carrier. For the detachment, a very thin CNT/GO layer was deposited between PI and glass carrier in order to reduce the peel strength [3]. The process of $\sim 1.5\text{-}\mu\text{m}$ -thick PI substrate was optimized. The gas barrier layer on the top of PI is a stack of alternate SiO_2 and SiN_x layers (a total of five layers starting with SiO_2) with a thickness of 25 nm each deposited by plasma-enhanced chemical vapor deposition (PECVD). The detailed fabrication process of a-IGZO TFT was described in [3]. TFT employs

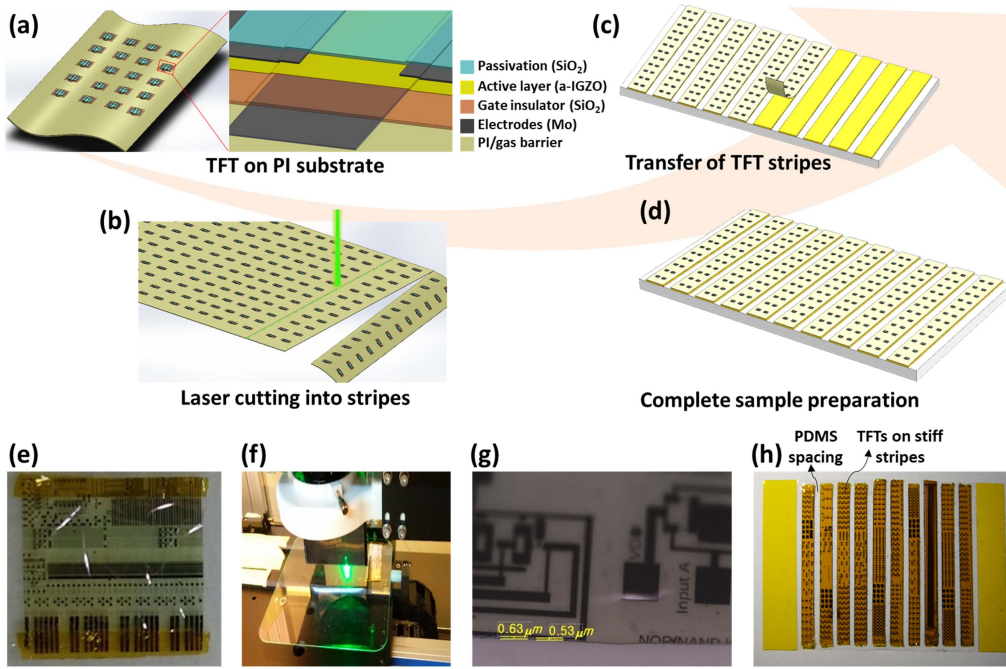


Fig. 2. Fabrication of stretchable a-IGZO TFTs. (a) Schematic of flexible a-IGZO TFTs on the PI substrate. The flexible devices were fabricated on PI/glass substrate and subsequently detached from the glass carrier. TFTs employ a BCE configuration (right). (b) Schematic of laser cutting to form stripe-shaped TFT membranes. (c) Transfer process of TFT stripes onto the prepared stiff-stripe/PDMS substrate. (d) Illustration of the stretchable sample after the complete fabrication process. (e) Photograph of the fabricated flexible a-IGZO TFTs free of wrinkling and curling after detachment. (f) Photograph of the green laser cutting system used to form stripe-shaped TFT membrane. (g) Optical image showing the laser cutting edge (width $< 1 \mu\text{m}$) remained on the TFT stripes. (h) Photograph of a-IGZO TFT membranes on stiff-stripe/PDMS substrate after the complete transfer process. The nonstretchable stripe region covers an area of $2.5 \text{ mm} \times 30 \text{ mm}$, whereas the PDMS spacing is $1.0 \text{ mm} \times 30 \text{ mm}$.

the conventional back-channel-etched (BCE) structure with a 20-nm-thick a-IGZO channel layer [Fig. 2(a)]. The bottom gate and source/drain electrodes are 100-nm-thick Mo by sputtering. The gate insulator and the passivation layer are PECVD SiO_2 with a thickness of 250 and 300 nm, respectively.

Fig. 2(e) shows a photograph of the flexible sample free of wrinkling and curling after detachment. The flexible membrane (a total thickness of $\sim 2 \mu\text{m}$) was cut into a stripe shape using a CO_2 laser system [Fig. 2(f)]. The laser beam (wavelength of 532 nm) can be positioned in tens of micrometers resolution offering fast, noncontact, and highly accurate cutting. Fig. 2(g) shows an optical image of the laser cutting edge on the TFT membrane. The width of the burning path was less than $1 \mu\text{m}$, indicating the capability of high resolution by laser cutting. The stripe-shaped TFT membranes were then transferred onto the stiff region on the PDMS substrate. Fig. 2(h) shows a photograph of the stretchable oxide TFTs after complete preparation steps.

C. Measurement Set-Up and Characterization

TFTs were measured in dark and at room temperature using an Agilent 4156C precision semiconductor parameter analyzer. TFT gate driver circuits were characterized using an Agilent DSOX2012A oscilloscope with load resistance and capacitance of $2 \text{ M}\Omega$ and 12 pF , respectively. TFTs and circuits were stretched using a home-designed machine.

For TFT characterization, the field-effect mobility (μ_{FE}) was derived from transconductance $g_m = \partial I_{\text{DS}} / \partial V_{\text{GS}}$, with $V_{\text{DS}} = 0.1 \text{ V}$. Subthreshold swing (SS) was taken as

$(d \log(I_{\text{DS}}) / dV_{\text{GS}})^{-1}$ of the range $10 \text{ pA} \leq I_{\text{DS}} \leq 100 \text{ pA}$, with $V_{\text{DS}} = 0.1 \text{ V}$. Turn-on voltage (V_{ON}) was taken as the gate voltage (V_{GS}) at which I_{DS} starts to monotonically increase with $V_{\text{DS}} = 0.1 \text{ V}$.

III. RESULTS AND DISCUSSION

A. Stretchability of Stiff-Stripe/PDMS Substrate

The thickness, optical transmittance in the visible range, and stretchability of the fabricated PDMS substrate are $\sim 45 \mu\text{m}$, $> 95\%$, and $\sim 220\%$ [Fig. 1(a) (inset)], respectively. The stretchability of stiff-stripe/PDMS substrate was evaluated by varying the width of stiff stripes. We define the stretch factor α by W/S , where “ W ” and “ S ” represent the width of the stiff stripe and soft spacing region [Fig. 3(a)], respectively. W of the stiff stripe is varied from 1 to 3 mm, whereas S is fixed at 1 mm. Fig. 3(b) shows a photograph of the prepared sample with $W = S = 1 \text{ mm}$ (α of 1), under a relaxed state. The stretched state of the sample is illustrated in Fig. 3(c). The stretching strain (ϵ) is calculated from the total length change of the entire substrate under relaxed and stretched states, i.e., the substrate that is initially 21-mm long is elongated up to 31.5 mm, corresponding to elastic stretching of 50%. Fig. 3(d) shows a photograph of the sample is stretched to 50% using the stretch machine. The shape of the stripes remains unchanged, whereas the spacing region (PDMS) is elongated, enabling the stretchability of the entire substrate. The array is assumed to be made of a series of n identical stripes and $n + 1$ spacing. Since the rigid stripe region is not deformable ($E_{\text{stripe}} = 2\text{--}2.5 \text{ GPa} \gg E_{\text{PDMS}} = 1.84 \text{ MPa}$), and that the

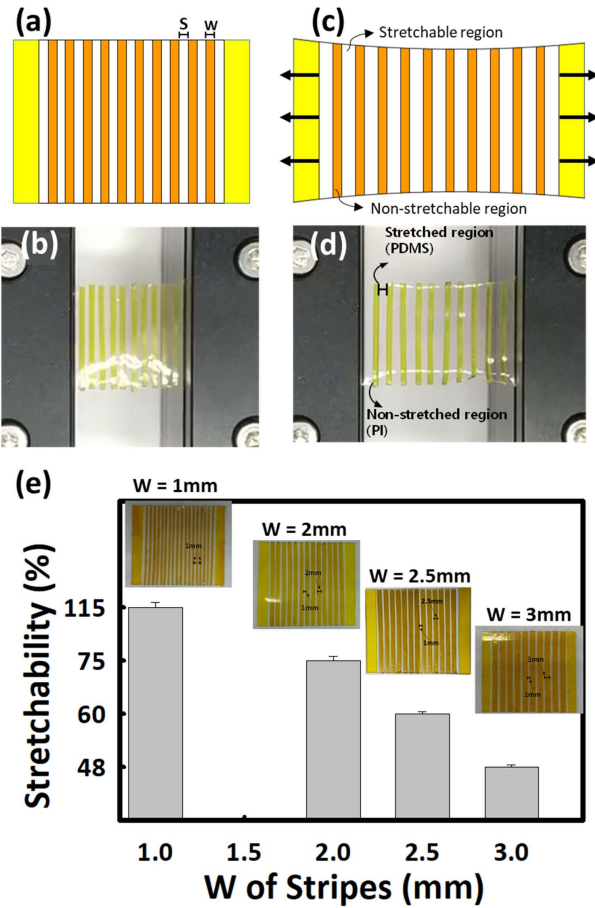


Fig. 3. Stretchability of stiff-stripe/PDMS substrate. (a) Schematic and (b) photograph of one sample with stripe width (W) of 1 mm and spacing (S) of 1 mm. (c) Schematic and (d) photograph of the sample being stretched using a home-designed stretch machine. W of the stripe region remains unchanged, whereas the spacing regions are elongated, enabling the stretchability of the entire substrate. (e) Stretchability of the stiff-stripe/PDMS substrate as a function of W of stripes, given a fixed S of 1 mm. The results are averaged from five tested samples.

soft spacing (PDMS) region is elongated to $S + \Delta S$ during stretching [23]. The stretching strain ε over the entire substrate can be described as

$$\begin{aligned} \varepsilon &= \frac{[nW + (n+1)(S + \Delta S)] - [nW + (n+1)S]}{nW + (n+1)S} \\ &= \frac{\Delta S}{\left(1 - \frac{1}{n+1}\right)W + S} \cong \frac{\Delta S}{W + S} \end{aligned} \quad (1)$$

when $n \gg 1$

The strain in the spacing region ($\varepsilon_{\text{spacing}}$) is

$$\varepsilon_{\text{spacing}} = \frac{\Delta S}{S} = \varepsilon \left(1 + \frac{W}{S}\right) = \varepsilon(1 + \alpha) \quad (2)$$

and

$$\varepsilon = \frac{\varepsilon_{\text{spacing}}}{1 + \alpha}. \quad (3)$$

Given that $\alpha = W/S = 1$ and maximum $\varepsilon_{\text{spacing}}$ (i.e., the stretchability of bare PDMS substrate) is $\sim 220\%$, the applied ε on the entire stiff-stripe/PDMS substrate can be calculated as $\sim 110\%$. Experimentally measured stretchability

is $\sim 115\%$ from the average results of five tested samples compared with the calculated value. The stretchability of the substrate was further tested with varying α factors. Fig. 3(e) shows stretchability of the stiff-stripe/PDMS substrate that can be tuned from $\sim 115\%$, 75%, 60% to 48%, respectively, by increasing W of stiff stripes from 1, 2, 2.5 to 3 mm, with fixed S of 1 mm (α varies from 1 to 3). The experimentally measured results are consistent with the calculated ones using (3). Considering the stripes with small W require more transfer times, while wider stripes limit the stretchability of the entire substrate, W of the stripes was chosen to be 2.5 mm, corresponding to α of 2.5, to guarantee the feasibility of transfer and the overall stretchability.

B. Stretchable a-IGZO TFTs

The nonstretchable stripe containing functional electronics covers an area of 2.5 mm \times 30 mm, whereas the stretchable spacing (PDMS) between the stripes is 1.0 mm \times 30 mm [Fig. 2(h)]. Electrical performance of the a-IGZO TFTs was tracked during detachment, laser cut, and transfer [Fig. 2(a)–(c)] onto the stiff-stripe/PDMS substrate. Negligible changes were found in device performance. The channel width (W) and length (L) are 20 and 11 μm , respectively. Overall, 10 a-IGZO TFTs on the stiff-stripe/PDMS substrate before stretching exhibit μ_{FE} of $17.2 \pm 1.8 \text{ cm}^2/\text{V}\cdot\text{s}$, V_{ON} of $0 \pm 0.5 \text{ V}$, and SS of $0.29 \pm 0.05 \text{ V}/\text{dec}$. The mobility of the a-IGZO TFTs herein is comparable with the reported oxide-based devices and is much higher than those of a-Si:H and organic TFTs [3], [10]. In addition, the excellent electrical stability, V_{ON} uniformity, and the mechanical flexibility of a-IGZO TFTs have been proven to be suitable for display backplane applications [26].

The stretchability of the a-IGZO TFTs was evaluated under various stretch conditions and cyclic tests. Fig. 4(a) and (b) shows the photographs of the a-IGZO TFTs under relaxed (0%) and 50% stretching conditions, respectively. The two ends of the sample are fixed in the stretch machine in such a way that the elongation can be performed perpendicular to the length direction of the stripes. Fig. 4(c) shows the evolution of the TFT transfer characteristics being exposed to various levels of strain from 0% (relaxed state), increased up to 50%, and return back to 0% (rerelaxed state). The corresponding evolutions of the extracted parameters are summarized in Table I. Changes in V_{ON} , SS, and μ_{FE} are $\pm 0.4 \text{ V}$, 0.09 V/dec, and $< 3.4\%$, respectively, during the stretching and relaxation procedures. No significant changes in TFT performance are found though the substrate is elongated by 1.5 times.

It has been reported that the mechanical strain experienced by oxide TFTs should stay well below $\approx 2\%$ in order to guarantee the electrical functionality and mechanical stability [7], [12]. a-IGZO TFTs herein are placed on stiff stripes transferred on the stretchable PDMS substrate. The electrical and mechanical stability during stretching is supposed to originate from the mechanical protection by using the stiff stripes. Romeo and Lacour [24] previously reported that the strain experienced by a-IGZO TFTs placed on SU-8 ($E_{\text{SU-8}} = 4 \text{ GPa}$) platform was close to 0% when the PDMS

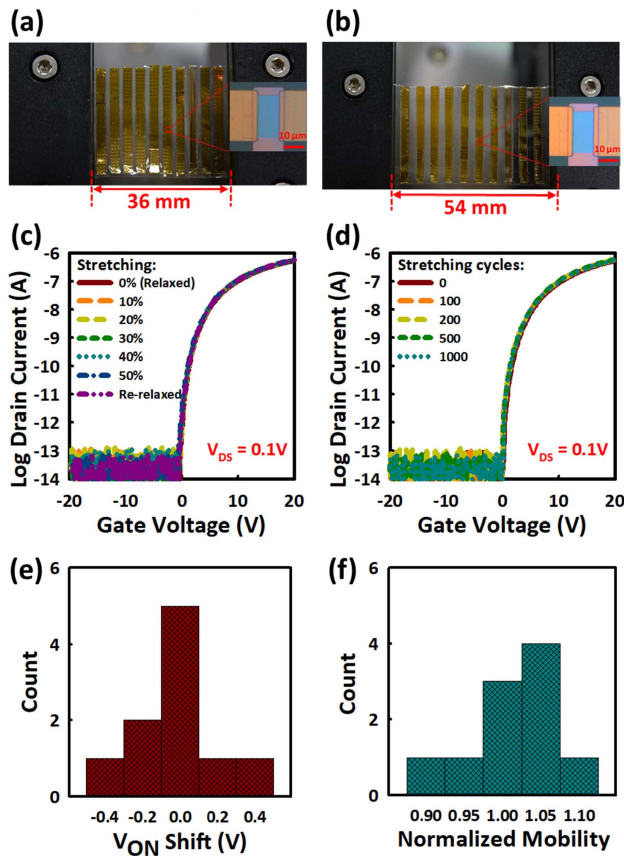


Fig. 4. Stretchable a-IGZO TFTs. Photographs of a-IGZO TFTs on stiff-stripe/PDMS substrate under (a) relaxed (0%) and (b) 50% stretching conditions using the stretch machine. Insets: optical images of a TFT taken under relaxed and 50% stretching states, respectively. (c) Evolution of the TFT transfer curves as a function of stretching strain. (d) Evolution of the transfer curves with the variation of repeated cycles of 50% stretching. (e) Turn-on voltage (V_{ON}) shift and (f) change in normalized field-effect mobility (μ_{FE}) of 10 TFTs measured after 50% stretching for 1000 repeated cycles. The parameter distributions exhibit that V_{ON} shifts within ± 0.4 V and μ_{FE} varies by $< \pm 7.4\%$. TFTs are with a channel width of $20 \mu\text{m}$ and length of $11 \mu\text{m}$.

substrate was stretched up to 20%. Na *et al.* [21] fabricated a-IGZO TFTs on $6\text{-}\mu\text{m}$ -thick patterned PI ($E_{PI} = 2.54$ GPa) islands on the PDMS substrate and maintained stable operation at 50% stretching. Hong *et al.* [22] analyzed the strain distribution using finite-element method (FEM) and found that the inorganic TFTs and LEDs located on PET ($E_{PET} = 2\text{--}2.7$ GPa) islands experienced negligible strains when the entire substrate was stretched up to 30%. Their fabricated temperature sensor remained as stable functions when being stretched to 50% [22]. The stripe region ($E_{stripe} = 2\text{--}2.5$ GPa) herein is >1000 times stiffer than the PDMS spacing region ($E_{PDMS} = 1.84$ MPa). The optical images shown in Fig. 4(a) and (b) (insets) reveal that there are no changes in the TFT under 50% stretching compared to that under relaxed states. Therefore, the stretching of the entire substrate mainly results in the elongation of the spacing region rather than in the stiff stripes. The strain distribution on the stiff region is well below the critical value, thus maintaining the stability of oxide TFTs by experiencing minimum strains during mechanical stretching. In addition, no crack or delamination was found from microscope images after the repeated stretching test.

TABLE I

EVOLUTION OF TFT PERFORMANCE: TURN-ON VOLTAGE (V_{ON}), ON-CURRENT (I_{ON}), OFF-CURRENT (I_{OFF}), ON-TO-OFF RATIO (I_{ON}/I_{OFF}), SS, AND FIELD-EFFECT MOBILITY (μ_{FE}) BEFORE STRETCHING (RELAXED), BEING STRETCHED AT DIFFERENT LEVELS OF STRAIN UP TO 50%, RETURN BACK TO RELAXED (RERELAXED) STATE, AND UNDER REPEATED STRETCHING TESTS AT 50% STRAIN

Items	V_{ON} (V)	μ_{FE} (cm^2/Vs)	SS (V/dec)	I_{ON} (μA)	I_{ON}/I_{OFF}
Relaxed (0%)	-0.1	17.27	0.33	5.5×10^{-7}	1.8×10^7
Stretching Strains (%)	10	-0.1	17.58	5.7×10^{-7}	1.1×10^7
	20	0.0	17.76	5.8×10^{-7}	2.9×10^7
	30	-0.2	17.79	5.8×10^{-7}	1.2×10^7
	40	-0.1	17.32	5.6×10^{-7}	2.8×10^7
	50	-0.4	17.84	5.9×10^{-7}	2.0×10^7
Re-relaxed	-0.2	17.91	0.40	5.9×10^{-7}	2.9×10^7
Repeated cycles (50% strain)	100	0.1	17.77	5.5×10^{-7}	2.7×10^7
	200	-0.1	18.10	5.6×10^{-7}	1.9×10^7
	500	-0.1	18.47	5.7×10^{-7}	2.8×10^7
	1000	-0.2	17.83	5.4×10^{-7}	1.4×10^7

This appears to be due to the small strain in the stiff region and the strong adhesion property of the tape [22], [28]. Note that the stiff stripes used for mechanical protections herein are low-cost and easily scalable for large-area applications.

Repeated stretching and relaxation were performed to test the robustness of stretchable a-IGZO TFTs. Fig. 4(d) demonstrates the evolution of the TFT transfer curves with varying stretch cycles. Changes in V_{ON} of ± 0.3 V, SS of ± 0.11 V, and μ_{FE} of $\pm 1.2 \text{ cm}^2/\text{V}\cdot\text{s}$ are found after 1000 stretching cycles (Table I). Ten TFTs with similar initial performances were tested and found fully functional after the repeated stretch (50% strain, 1000 cycles). Fig. 4(e) and (f) shows the variations in V_{ON} and normalized mobility of the 10 TFTs are within ± 0.4 V and 7.4%, respectively. This once again confirms the mechanical protection and strong adhesion by using the stiff stripes. The TFTs currently can be repeatedly stretched to 50% along one direction. An array of stiff-stripes with soft PDMS spacing in both directions would enable the stretchability in the transverse direction. The TFTs can be stable and stretched to a maximum strain of $\sim 70\%$ before permanent disconnections occur in the soft spacing close to the edge of the rigid stripe, where a peak strain is located from FEM analysis and strain measurement [11], [24]. To further improve the stretchability, stretchable substrate with lower Young's modulus [29], [30], larger soft spacing, and gradients stiffness of the rigid platforms [11] would be considered.

C. Stretchable a-IGZO TFT-Based Circuits

The a-IGZO TFT-based inverter and gate driver circuits were fabricated and characterized on the stiff-stripe/PDMS substrate [Fig. 2(h)]. Fig. 5(a) shows the circuit diagram (left)

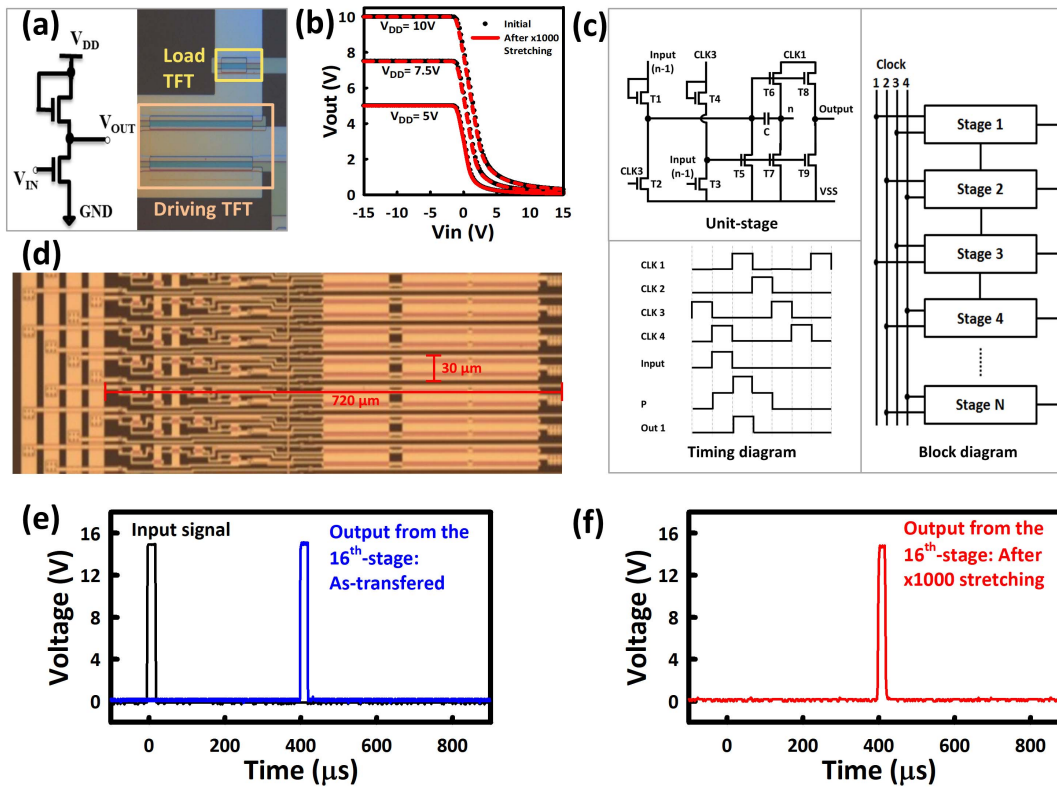


Fig. 5. Stretchable a-IGZO TFT-based circuits. (a) Circuit schematic (left) and optical image (right) of the fabricated inverter. (b) VTCs of the inverter for various V_{DD} 's. (c) Block diagram of a single stage (top left), timing diagram (bottom left), and schematic (right) of a gate driver circuit. (d) Optical image of the fabricated gate driver circuits with 30- μm pitch. (e) Input signal (black) and the output waveform (blue) from the last stage of the fabricated gate driver circuit before the stretch test. (f) Output waveform (red) of the last stage after the repeated stretch test. The supply voltage was 15 V. Negligible changes are found after 50% stretching for 1000 cycles.

and optical image (right) of an enhancement-load-type inverter. The load and driving TFTs, respectively, have W of 60 and 480 μm , whereas L is fixed at 10 μm . This gives an ideal gain of 2.83 calculated from the square root of β ratio, the ratio of channel W of driving to load TFTs [31]. The initial voltage transfer characteristics (VTCs) of the inverter are indicated by black circular dots in Fig. 5(b). Good level conversions are obtained at various supply voltages (V_{DD} 's). The gains calculated from the slopes of VTCs are 2.20, 2.26, 2.32, respectively, for the V_{DD} 's of 5, 7.5, and 10 V, which are comparable to the ideal gain value. VTCs after 1000 stretching cycles (50% strain) are plotted together as shown in Fig. 5(b)(red solid lines). No significant changes are found compared to that of the initial performance. The static gains are 2.23, 2.28, and 2.35, respectively, with increasing V_{DD} 's.

Fig. 5(c) shows the schematic circuit design (left top), timing diagram (left bottom), and block diagram (right) of a 16-stage gate driver based on a-IGZO TFTs. The circuit design employs nonoverlapping four-phase clock signals (CLK1–CLK4) with a 25% duty cycle. A single stage of the gate driver consists of nine TFTs (T1–T9) and one capacitor (C); Each stage of the circuits provides two separate output nodes, one for the next stage (“n” node) and the other one (“Output” node) for driving the display panel. This design can improve the yield of fabricated gate drivers by reducing the process influences, such as contaminants or particles. Detailed

design and the operation of the gate driver can be found in our previous report [32]. L of all TFTs was fixed at 4 μm , whereas W values were optimized through SmartSpice simulation.

Fig. 5(d) shows an optical image of the fabricated gate driver circuits. A single stage occupies an area of 30 $\mu\text{m} \times 720 \mu\text{m}$ which makes it suitable for high-resolution and narrow-bezel displays. Fig. 5(e) shows the input and output waveform of the gate driver circuit as-transferred on the stiff-stripe/PDMS substrate (relaxed state). The input signal has an amplitude of 15 V and a pulsewidth of 20 μs . The high output voltage (V_H), rise time (T_r), and fall time (T_f) are, respectively, ~ 14.7 V, 0.62 μs , and 0.46 μs , which are comparable with the reported results in the literature [32]. Note that the gate driver circuits herein were fabricated on ultrathin (1.5 μm) PI substrate, and measured on the stiff-stripe/PDMS substrate. Fig. 5(f) shows the circuit performance after 1000 stretching cycles (50% strain). No significant degradations are found from the last stage output waveforms, giving the V_H , T_r , and T_f of 14.6 V, 0.78 μs , and 0.67 μs , respectively. No cracks are found in the TFTs and metal lines after repeated test through the microscopes. These results indicate that all 144 TFTs and metal lines in the fabricated gate driver circuits are functioning well during the repeated mechanical stretching. This proves the feasibility of employing the high-performance oxide TFT-based gate drivers for stretchable display applications.

TABLE II
COMPARISON OF THIS PAPER WITH THE STATE-OF-THE-ART HYBRID STRETCHABLE TFTs USING STIFF PLATFORMS

Substrate	Stiff platform, Patterning	Feature size (shape, S)	Adhesion (stiff platform-substrate)	TFT channel, Mobility (cm ² /Vs)	Integrated functionality	Stretchability	Ref.
PDMS	Si/SU-8 islands	200 μm islands, S: N/A	N/A	single-crystal Si, >700	8×8 AM-LED display (1060 μm pitch) TFTs	40% for 200 cycles	1
PDMS	SU-8, UV lithography	1.5 mm islands, S = 4.5 mm	Embedded	IGZO, 2.64		20%	24
PDMS	SU-8, UV lithography	~500 μm islands, S: N/A	N/A	IGZO, <15	TFTs	5% for 100 cycles	25
PDMS	PI	~1 mm islands, S: N/A	PDMS capping	IGZO, ~1.3	4×4 TFT array	40%	17
PDMS	PI, photolithography	~1mm islands, S ~0.5 mm	van der Waals forces + top PI	SWCNT, 4.51 ± 1.67	Memory units, logic gates	20% for 1000 cycles	18
PDMS	PI, photolithography	Islands, S: N/A	O ₂ plasma treatment	IGZO, 6.1	TFTs	49%	20, 21
PDMS	PI, cut	Islands, S: N/A	N/A	Pentacene, 0.48	Nonvolatile memory Active matrix (19 × 37 TFTs)	50 70% for 30 cycles	35
PDMS	PI + stiff PDMS by UV exposure	2mm islands, S = 6 mm	Gradient stiff-to-soft interface	Pentacene, 0.105	TFTs	12.6 %	19
PDMS	PI + stiff PDMS, laser cutting	Circular islands, S: N/A	Oxygen plasma treatment	DNTT, 1.8	2×2 TFTs array	110%	34
PDMS	DLC, shadow mask	200 μm islands, S = 400 μm	Direct adhere	N/A	N/A	30%	23
PDMS	Alumina platelets, magnetic response	30 μm wide stripe, S = 120 μm	Embedded	IGZO, ~9	TFT arrays	20% (substrate stretch)	33
PDMS	Graded stiff patches	~5 mm islands, S: N/A	60 μm-thick adhesive	IGZO, ~11.3	Amplifier, rectifier circuit	120% for 1 cycle, 70% for 1000 cycles	7
Ecoflex	PET	1cm islands, S = 1 mm	PDMS capping	SWCNT, 6.7 ± 4.0	5×5 AM LED array, temp. sensor array	50%	22
Ecoflex+	Stiff PDMS, mold pattern	1 cm islands, S = 0.2 cm	Curing	SWCNT, unknown	LEDs array, SnO ₂ -NW sensors, TFT	30%	29
PDMS-b-PEO + BP	Stiff PDMS, UV exposure	1 cm islands, S = 1.5/1.2 cm	Embedded	Pentacene, 0.01	TFT	200%	30
PDMS	Stiff adhesive, laser cutting	2.5 mm × 1.0 mm stripe, S = 1.0 mm	Adhesive	IGZO, 17.2 ± 1.8	TFT arrays, gate driver circuits	50% for 1000 cycles	This work

*Shape, S: shape of the stiff platform, width of the spacing region between adjacent stiff platforms.

SWCNT: single-walled carbon nanotubes, DNTT: (dinaphtho[2,3-b:20,30-f]thieno[3,2-b]thiophene), AM LED: active matrix light-emitting diode.

Compared with the state-of-the-art hybrid stretchable TFTs using stiff platforms (Table II), this approach employs commercially available adhesive tapes that provide excellent adhesion and mechanical protections of brittle electronics following a simple transfer process. The design of stiff stripes is suitable for the integration of complicated electronic systems. Especially the number of external control lines can be significantly reduced, whereas the flexibility and yield can be further improved by the integration of TFT-based gate driver circuits. This approach is practical by taking advantage of the mature fabrication process and high-performance oxide devices. A combination of high-performance integrated display on each stiff stripe and highly stretchable conductors interconnecting the stiff stripes can lead to a stretchable display system. Although the stretchable interconnects are beyond the scope of discussion in this paper, there have been numerous methods to fabricate stretchable interconnects with excellent electric conductivity and mechanical durability on elastic substrates [1], [2], [36]. This technology can be used for the practical stretchable displays with high-resolution over a large area.

IV. CONCLUSION

In conclusion, we report high-performance a-IGZO TFTs and circuits transferred on the stripe-shaped stiff platform

on stretchable PDMS substrate. Commercially available adhesive and rigid tapes are employed for strong adhesion and mechanical protection of brittle electronics. The fabricated a-IGZO TFTs and gate driver circuits can be repeatedly stretched up to 50% without delamination and significant performance degradation. This approach is low cost, easily scalable and reproducible and thus can be used for achieving stretchable displays by taking advantage of the mature fabrication process and high-performance oxide devices.

REFERENCES

- [1] M. Choi *et al.*, "Stretchable active matrix inorganic light-emitting diode display enabled by overlay-aligned roll-transfer printing," *Adv. Funct. Mater.*, vol. 27, no. 11, Mar. 2017, Art. no. 1606005. doi: [10.1002/adfm.201606005](https://doi.org/10.1002/adfm.201606005).
- [2] T. Sekitani *et al.*, "Stretchable active-matrix organic light-emitting diode display using printable elastic conductors," *Nature Mater.*, vol. 8, pp. 494–499, May 2009. doi: [10.1038/NMAT2459](https://doi.org/10.1038/NMAT2459).
- [3] Y.-H. Kim, E. Lee, J. G. Um, M. Mativenga, and J. Jang, "Highly robust neutral plane oxide TFTs withstanding 0.25 mm bending radius for stretchable electronics," *Sci. Rep.*, vol. 6, no. 11, p. 25734, May 2016. doi: [10.1038/srep25734](https://doi.org/10.1038/srep25734).
- [4] J. Lee *et al.*, "5.8-inch QHD flexible AMOLED display with enhanced bendability of LTPS TFTs," *J. Soc. Inf. Display*, vol. 26, no. 4, pp. 200–207, Apr. 2018. doi: [10.1002/jsid.655](https://doi.org/10.1002/jsid.655).
- [5] Y.-C. Jeong, "Late-news poster: Flexible cover window for foldable display," *SID Symp. Dig. Tech. Papers*, vol. 49, no. 1, pp. 1921–1924, May 2018. doi: [10.1002/sdtp.12474](https://doi.org/10.1002/sdtp.12474).

- [6] C.-C. Lee and Y.-Y. Liou, "Dependent analyses of multilayered material/geometrical characteristics on the mechanical reliability of flexible display devices," *IEEE Trans. Device Mater. Rel.*, vol. 18, no. 4, pp. 639–642, Dec. 2018. doi: [10.1109/TDMR.2018.2878485](https://doi.org/10.1109/TDMR.2018.2878485).
- [7] N. Münzenrieder *et al.*, "Stretchable and conformable oxide thin-film electronics," *Adv. Electron. Mater.*, vol. 1, no. 3, Mar. 2015, Art. no. 1400038. doi: [10.1002/aelm.201400038](https://doi.org/10.1002/aelm.201400038).
- [8] T. Sekitani and T. Someya, "Stretchable organic integrated circuits for large-area electronic skin surfaces," *MRS Bull.*, vol. 37, pp. 236–245, Mar. 2012. doi: [10.1557/mrs.2012.42](https://doi.org/10.1557/mrs.2012.42).
- [9] B. K. Sharma and J.-H. Ahn, "Flexible and stretchable oxide electronics," *Adv. Electron. Mater.*, vol. 2, no. 8, Aug. 2016, Art. no. 1600105. doi: [10.1002/aelm.201600105](https://doi.org/10.1002/aelm.201600105).
- [10] S. Wang *et al.*, "Skin electronics from scalable fabrication of an intrinsically stretchable transistor array," *Nature*, vol. 555, no. 7694, pp. 83–88, 2018. doi: [10.1038/nature25494](https://doi.org/10.1038/nature25494).
- [11] N. Naserifar, P. R. LeDuc, and G. K. Fedder, "Material gradients in stretchable substrates toward integrated electronic functionality," *Adv. Mater.*, vol. 28, no. 18, pp. 3584–3591, May 2016. doi: [10.1002/adma.201505818](https://doi.org/10.1002/adma.201505818).
- [12] M.-J. Park *et al.*, "Improvements in the bending performance and bias stability of flexible InGaZnO thin film transistors and optimum barrier structures for plastic poly(ethylene naphthalate) substrates," *J. Mater. Chem. C*, vol. 3, no. 18, pp. 4779–4786, Apr. 2015. doi: [10.1039/c5tc00048c](https://doi.org/10.1039/c5tc00048c).
- [13] T. Q. Trung and N.-E. Lee, "Materials and devices for transparent stretchable electronics," *J. Mater. Chem. C*, vol. 5, no. 9, pp. 2202–2222, 2017. doi: [10.1039/c6tc05346g](https://doi.org/10.1039/c6tc05346g).
- [14] D.-H. Kim *et al.*, "Stretchable and foldable silicon integrated circuits," *Science*, vol. 320, no. 5875, pp. 507–511, Apr. 2008. doi: [10.1126/science.1154367](https://doi.org/10.1126/science.1154367).
- [15] S. Wang, Y. Huang, and J. A. Rogers, "Mechanical designs for inorganic stretchable circuits in soft electronics," *IEEE Trans. Compon., Packag., Manuf. Technol.*, vol. 5, no. 9, pp. 1201–1218, Sep. 2015. doi: [10.1109/TCPMT.2015.2417801](https://doi.org/10.1109/TCPMT.2015.2417801).
- [16] G. Cantarella *et al.*, "Buckled thin-film transistors and circuits on soft elastomers for stretchable electronics," *ACS Appl. Mater. Interfaces*, vol. 9, no. 34, pp. 28750–28757, Aug. 2017. doi: [10.1021/acsami.7b08153](https://doi.org/10.1021/acsami.7b08153).
- [17] C. W. Park, J. B. Koo, C.-S. Hwang, H. Park, S. G. Im, and S.-Y. Lee, "Stretchable active matrix of oxide thin-film transistors with monolithic liquid metal interconnects," *Appl. Phys. Express*, vol. 11, no. 12, Oct. 2018, Art. no. 126501. doi: [10.7567/APEX.11.126501](https://doi.org/10.7567/APEX.11.126501).
- [18] D. Son *et al.*, "Stretchable carbon nanotube charge-trap floating-gate memory and logic devices for wearable electronics," *ACS Nano*, vol. 9, no. 5, pp. 5585–5593, Apr. 2015. doi: [10.1021/acs.nano.5b01848](https://doi.org/10.1021/acs.nano.5b01848).
- [19] I. M. Graz, D. P. J. Cotton, A. Robinson, and S. P. Lacour, "Silicone substrate with in situ strain relief for stretchable thin-film transistors," *Appl. Phys. Lett.*, vol. 98, no. 12, Mar. 2011, Art. no. 124101. doi: [10.1063/1.3570661](https://doi.org/10.1063/1.3570661).
- [20] S.-W. Jung, J. B. Koo, C. W. Park, B. S. Na, J.-Y. Oh, and S. S. Lee, "Fabrication of stretchable organic-inorganic hybrid thin-film transistors on Polyimide stiff-island structures," *J. Nanosci. Nanotechnol.*, vol. 15, no. 10, pp. 7526–7530, Nov. 2015. doi: [10.1166/jnn.2015.11151](https://doi.org/10.1166/jnn.2015.11151).
- [21] B. S. Na *et al.*, "Ingazno-based stretchable ferroelectric memory transistor using patterned polyimide/polydimethylsiloxane hybrid substrate," *J. Nanosci. Nanotechnol.*, vol. 16, no. 10, pp. 10280–10283, Oct. 2016. doi: [10.1166/jnn.2016.13144](https://doi.org/10.1166/jnn.2016.13144).
- [22] S. Y. Hong *et al.*, "Stretchable active matrix temperature sensor array of polyaniline nanofibers for electronic skin," *Adv. Mater.*, vol. 28, no. 5, pp. 930–935, Feb. 2016. doi: [10.1002/adma.201504659](https://doi.org/10.1002/adma.201504659).
- [23] S. P. Lacour, S. Wagner, R. J. Narayan, T. Li, and Z. I. Suo, "Stiff subcircuit islands of diamondlike carbon for stretchable electronics," *J. Appl. Phys.*, vol. 100, no. 1, Apr. 2006, Art. no. 014913. doi: [10.1063/1.2210170](https://doi.org/10.1063/1.2210170).
- [24] A. Romeo and S. P. P. Lacour, "Stretchable metal oxide thin film transistors on engineered substrate for electronic skin applications," in *Proc. 37th Annu. Int. Conf. IEEE Eng. Med. Biol. Soc. (EMBC)*, Aug. 2015, pp. 8014–8017. doi: [10.1109/EMBC.2015.7320252](https://doi.org/10.1109/EMBC.2015.7320252).
- [25] B. K. Sharma *et al.*, "Load-controlled roll transfer of oxide transistors for stretchable electronics," *Adv. Funct. Mater.*, vol. 23, no. 16, pp. 2024–2032, Apr. 2013. doi: [10.1002/adfm.201202519](https://doi.org/10.1002/adfm.201202519).
- [26] E. Fortunato, P. Barquinha, and R. Martins, "Oxide semiconductor thin-film transistors: A review of recent advances," *Adv. Mater.*, vol. 24, no. 22, pp. 2945–2986, Jun. 2012. doi: [10.1002/adma.201103228](https://doi.org/10.1002/adma.201103228).
- [27] S. Wagner and S. Bauer, "Materials for stretchable electronics," *MRS Bull.*, vol. 37, no. 3, pp. 207–213, Mar. 2012. doi: [10.1557/mrs.2012.37](https://doi.org/10.1557/mrs.2012.37).
- [28] N. Lu, J. Yoon, and Z. Suo, "Delamination of stiff islands patterned on stretchable substrates," *Int. J. Mater. Res.*, vol. 98, no. 8, pp. 717–722, Jun. 2007. doi: [10.3139/146.101529](https://doi.org/10.3139/146.101529).
- [29] J. Yoon, S. Y. Hong, Y. Lim, S.-J. Lee, G. Zi, and J. S. Ha, "Design and fabrication of novel stretchable device arrays on a deformable polymer substrate with embedded liquid-metal interconnections," *Adv. Mater.*, vol. 26, no. 38, pp. 6580–6586, Oct. 2014. doi: [10.1002/adma.201402588](https://doi.org/10.1002/adma.201402588).
- [30] S. Gandla, H. Gupta, A. R. Pininti, A. Tewari, and D. Gupta, "Highly elastic polymer substrates with tunable mechanical properties for stretchable electronic," *RSC Adv.*, vol. 6, no. 109, pp. 107793–107799, Nov. 2016. doi: [10.1039/C6RA20428G](https://doi.org/10.1039/C6RA20428G).
- [31] X. Li, D. Geng, M. Mativenga, and J. Jang, "High-speed dual-gate a-IGZO TFT-based circuits with top-gate offset structure," *IEEE Electron Device Lett.*, vol. 35, no. 4, pp. 461–463, Apr. 2014. doi: [10.1109/LED.2014.230566](https://doi.org/10.1109/LED.2014.230566).
- [32] D. Geng, Y. F. Chen, M. Mativenga, and J. Jang, "30 μ m-pitch oxide TFT-based gate driver design for small-size, high-resolution, and narrow-bezel displays," *IEEE Electron Device Lett.*, vol. 36, no. 8, pp. 805–807, Aug. 2015. doi: [10.1109/LED.2015.2445319](https://doi.org/10.1109/LED.2015.2445319).
- [33] R. M. Erb *et al.*, "Locally reinforced polymer-based composites for elastic electronics," *ACS Appl. Mater. Interfaces*, vol. 4, no. 6, pp. 2860–2864, Jun. 2012.
- [34] N. Matsuhiwa *et al.*, "Printable elastic conductors with a high conductivity for electronic textile applications," *Nature Commun.*, vol. 6, p. 7461, Jun. 2015. doi: [10.1038/ncomms8461](https://doi.org/10.1038/ncomms8461).
- [35] T. Sekitani, Y. Noguchi, K. Hata, T. Fukushima, T. Aida, and T. Someya, "A rubberlike stretchable active matrix using elastic conductors," *Science*, vol. 321, no. 5895, pp. 1468–1472, Sep. 2008.
- [36] G. Li, X. Wu, and D.-W. Lee, "Selectively plated stretchable liquid metal wires for transparent electronics," *Sens. Actuators B, Chem.*, vol. 221, pp. 1114–1119, Dec. 2015. doi: [10.1016/j.snb.2015.07.062](https://doi.org/10.1016/j.snb.2015.07.062).